Transactions of the **14th International Conference on Structural Mechanics in Reactor Technology** (SMiRT 14), Lyon, France, August 17-22, 1997

GW/8

Crack effects on the fracture behaviour in the duplex steels

Kozak V.(1), Dlouhy I.(1), Holzmann M.(2)
(1) Institute of Physics of Materials, Czech Republic
(2) Institute of Physical Metallurgy, Czech Republic

ABSTRACT Fracture behaviour of duplex stainless steel taken from thick wall pipe was analysed and fracture mechanics tests were carried out in transition region. Accepting the Beremin approach to the analysis of brittle failure the local fracture parameters have been calculated using FEM for Charpy type and notched tensile specimen. Two microstructures have been selected for this presentation - as received and after model embrittlement. Weibull stresses (location parameters) were related to fractographic features and tested by fracture toughness prediction for pre-cracked specimen. Critical fracture stresses were determined for Charpy type specimen at static three point bending and low blow impact testing. Correlation with tensile stress distribution below notch was found out.

1. INTRODUCTION

Although known for many years, it is only since the 80ies the duplex stainless ferritic-austenitic steels (DSS) became popular [1,2,3,4]. DSS possess higher strength and corrosion resistance than austenitic stainless steels, therefore, they are increasingly replacing in situations from chemical plant to offshore oil and gas applications [5]. Critical welds in the offshore industry must have sufficient toughness at temperatures as low as -50°C [6]. The thermal cycle in the weld and HAZ can cause the precipitation of a number of detrimental phases [7,8]. Of these, reformation of the ferrite to α' by spinodal decomposition between 500°C and 250°C results in “475°C embrittlement”. For service applications of steels which involve temperatures below ambient, it is normal practice to minimise the risk of brittle failure by imposing impact test requirements. For ferritic steels, the Charpy impact energy and/or other fracture characteristics required are standardised. For DSS there is still a lot of uncertainty in assessment criteria of low temperature toughness and the ferrite embrittlement.

Transferability of fracture toughness values obtained on small laboratory test specimen raises the problem of geometrical and size effects. Although sharp stress gradient occurs below the V notch the Charpy type specimens seems to be suitable for local parameters determination of the DSS.

As shown in [9] for example brittle failure probability of arbitrary cell inside the process zone is controlled by applied stress σ,

$$P_f = (\sigma/\sigma_u)^m \,, \tag{1}$$

where m is Weibull shape parameter characterising microscopic fracture behaviour, and σ_u is Weibull location parameter, a stress which represents the intrinsic resistance of the material to cleavage fracture. Cumulative probability of failure can be found introducing the Weibull stress into the above equation,

$$P_f = 1 - \exp\{-(\sigma_w/\sigma_u)^m\}. \quad (2)$$

The stress σ_w is given [9] by expression

$$\sigma_w = \{\Sigma\, \sigma_1{}^m(\Delta V/V_0)\}^{1/m}. \quad (3)$$

ΔV is a volume in which the principal stress σ_1 is acting and it is usually determined by the corresponding mesh element used by FEM. The integration is evaluated over plastically deformed elements on premise that microcracks are not created in the cells residing outside the crack-tip plastic zone. The cell volume V_0 can be chosen in the order of about ten grain sizes in case the cleavage fracture micromechanism is dominating [11]. Parameters σ_u and m are considered to be transferable local material properties, independent of temperature, geometry or loading mode. Microstructural aspects in relation to parameters σ_u and m need further explanation. For DSS relatively small attention has been paid to the CVN bend specimen from this point of view.

The aim of the paper can be seen in experimental verification of the microstructural nature of cleavage fracture stress and location parameter for two different model microstructures. The independence of critical fracture stress on temperature and strain rate should be also proved. The susceptibility of local parameters to steel microstructure should be discussed.

2. MATERIAL, EXPERIMENTAL AND CALCULATION PROCEDURES

Material characterisation

The steel used had a chemical composition (wt %): 0.022 C; 1.07 Mn; 0.25 Si; 4.98 Ni; 21.5 Cr; 3.1 Mo; 0.118 N; 0.035 P; 0.012 S. The steel was commercially produced forged thick wall pipe (outer diameter of 700 mm, wall thickness of 80 mm). Two microstructures were selected for this investigation: (i) initial state (as received) after solution annealing and (ii) aged state after ageing 5 h at 475 °C. Selected materials characteristics are shown in Table 1. In this Table, the value of d_{AG} represents average austenitic grain size, d_{FG} is average ferritic grain size.

Table 1: Microstructural and selected mechanical characteristics of materials studied

micro-structure	annealing	HV10	d_{AG} [μm]	d_{FG} [μm]	$R_p0.2$ [MPa]	R_m [MPa]	CVN imp. energy [J]	DBTT [°C]
as rec		242	49±11	38±17	468	619	198	-45
aged	475°C/5h	211			587	762	193	5

Mechanical properties

The tensile properties have been measured using the cylindrical specimens with diameter of 6 mm, testing was realized over temperature range of -196 to +100 °C at a cross - head speed of 2 mm.min^{-1}. The yield strength was taken to be the 0.2 % proof stress.

Charpy type specimens were tested under the two types of loading: (i) CVN impact energies were measured using instrumented impact tester over a temperature range of -196 to 200 °C and ductile to brittle transition temperatures (DBTT) have been determined among others. To obtain data for critical fracture stress determination, the fracture force, F_{FR}, and general yield force, F_{GY}, have been taken from load deflection records. (ii) The same approach was used for CVN specimen in static three point bending. For one selected temperature in lower shelf region (below temperature t_{GY} at which conincidence of F_{FR} and F_{GY} on their temperature dependences occurs, see Table 2) a range of specimens was tested to obtain data for statistical treatment.

Axisymmetrically notched tensile specimens with diameter of 16 mm were also tested (at temperatures given in Table 2) to generate data for local parameter calculation. The Charpy type geometry of the notch was machined circumferencially, the minimum specimen diameter in notch root section being 8 mm. Cross sectional in notch root plane and longitudinal changes of specimen have been measured using special transducers.

Fracture toughness values were measured using standard CT specimen tested at 1mm/min displacement rate over temperature range from -196 C to +50 °C.

The fracture appearance and fracture micromorphology of broken CVN specimen and etched microstructures in section perpendicular to fracture surfaces were assessed using SEM. The complete material analysis is out of scope of the paper and will be given elsewhere [12].

Calculation procedures

For test temperature below t_{GY} (see Table 2) the principal stress distribution below the notch was calculated for fracture forces measured. A 2D model under plane strain conditions was used for the elastic-plastic analysis using symmetry of the three point bending of V-notched specimen [13]. Axi-symmetric model for notch tensile specimen was applied. Finite elements package ANSYS 5.3 was used for calculations.

Table 2: Experimental material characteristics and data used in FEM calculations

	test temp. [°C]	$R_p0.2$ [MPa]	$R_p0.1$ [MPa]	σ_y [MPa]	E [MPa]	ν	
as rec	-175	1050	972	870	2.05e5	0.3	Charpy
as rec	-120	885	840	740	2.05e5	0.3	tensile
aged	-140	1070	985	840	2.05e5	0.3	Charpy
aged	-80	901	825	690	2.05e5	0.3	tensile

Accepting the Beremin approach to the analysis of local criterion for cleavage fracture the location parameters for Charpy type specimen were calculated. The flow behaviour was computed using incremental plasticity (with Von Mises criterion). The attention was paid to the implementation of the true stress - true strain curve. These were approximated using 5 points (multilinear approximation). To prove the validity of FEM calculation the load - displacement curves were computed and compared with the experimentally obtained traces. As mentioned above, standard finite element computer code for strain and stress distribution around the notch was used. Then the Weibull shape parameter, m, and Weibull stress, σ_w, were determined by integration in the plastic zone ahead of the crack tip for estimated values of characteristic cell V_0. From the plot of calculated probability vs σ_w the Weibull parameter m can be modified. Once the value of m has been determined, the value of location parameter, σ_u, is read from the linear regression for P_f =0.63. Similar procedure was applied for determinating of local parameters for notched tensile specimens.

3. DESCRIPTION OF RESULTS

Microstructure and basic mechanical properties

The microstructure of DSS from thick wall pipe is typical by comparable amount of ferrite and austenite crystals both being without preferential orientation. Summary of basic mechanical properties generated at ambient temperature is given in Table 1. High isotropy but inhomogeneity of mechanical properties was found out for this material [14].

At tensile loading the yield stress is controlled by the harder ferrite phase. Yield of initial states at lower temperatures and age hardened steels is accompanied by deformation twinning and slip band formation in the ferrite. The fracture transition behaviour and brittleness of ferrite is compensated by austenite no embrittlement phenomena could be observed.

For both as received and aged condition and for radial direction of specimen axis typical temperature dependencies of yield strength and Charpy impact energy are given in Fig. 1. The dependencies of yield strength with temperature are similar as in standard steels. An exponential fit seems to be the best for experimental data. Model age-hardening results in remarkable increase of tensile properties as it can be seen from the shift between both curves.

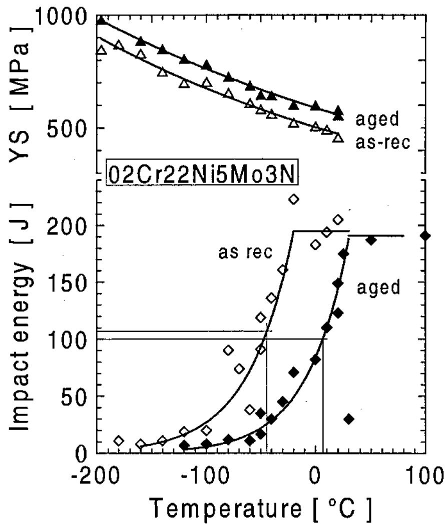

Figure 1 : Temperature dependencies of yield strength and Charpy impact energy for initial and aged material.

Local parameters and FEM calculations

For both notched specimens used the tensile stress distribution below notch has been calculated to simulate the stress state at fracture. Large strain and displacement effects were included to obtain the best possible estimation of the stress and strain distribution. Six-node quadrilateral axi-symmetric elements were applied (Plane 2). The mesh contained at least 10 elements at the notch tip diameter. Fig. 2a shows family of principal stress distributions at fracture forces obtained for Charpy type specimen (the notch beeing oriented left in figure) by testing at one temperature. Similar distribution are introduced for steel after age hardening in Fig. 3a. For comparison in both figures are given principal stress distributions calculated for fracture forces of notched tensile specimen tested at one temperature (Figs 2b and 3b). Three findings follow from comparison of tensile stress distributions. (i) Comparable values of maximum principal stress below notch for both types of notched specimen used. (ii) Smaller stress gradient observed in notched tensile specimen, it means the higher volume sampled giving material information about fracture condition. (iii) Slightly higher maximum stresses observed in both specimen types for steel being after age hardening.

Based on fracture parameters of above characterised sets of specimens the local parameters, σ_u and m, were determined. The calculations were applied for various cell size V_0, represented in this work by parameter λ, $\lambda = (V_0)^{1/3}$. A summary of representative results of calculations is introduced in Figs. 4 and 5 and Table 3.

Allowing for the variation of location parameter, σ_u, with cell size V_0 and the shape of cumulative probability curve, the following findings can be summarised: (i) The local parameters σ_u and m are well susceptible and different for the both microstructures investigated. The value σ_u, higher for aged material when compared with as-received state, corresponds to relation of maximum tensile stresses below notch and corresponding yield

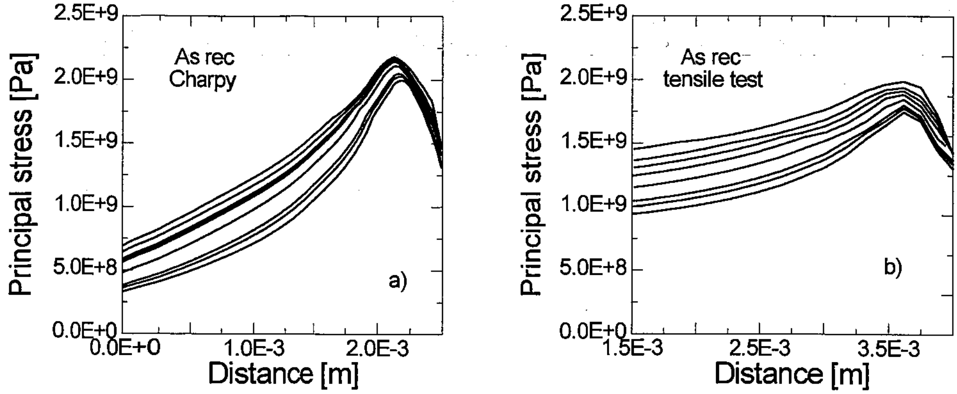

Figure 2: As received steel, principal stress distribution below notch (left) calculated for fracture forces of specimens tested at one temperature a) Charpy type specimens tested in static bending b) notched tensile specimens.

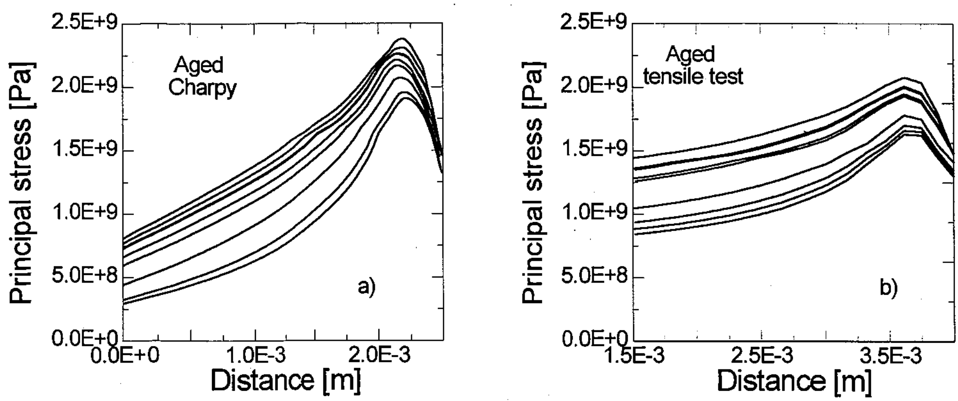

Figure 3: Steel after age hardening, principal stress distribution below notch (left) calculated for fracture forces of specimens tested at one temperature a) Charpy type specimens tested in static bending b) notched tensile specimens.

Table 3: Local parameters calculated for various cell size and for both specimen geometries.

micro-structure	test	m	λ= 50 μm σ_u [MPa]	λ=100 μm σ_u [MPa]	λ=150 μm σ_u [MPa]	λ=200 μm σ_u [MPa]	λ=400 μm σ_u [MPa]
as rec	Charpy	25.6	2904	2675	2560	2465	2280
as rec	tensile	18.0	2660	2380	2240	2140	1890
aged	Charpy	13.4	4360	3728	3415	3195	2710
aged	tensile	10.1	3745	3150	2780	2560	2090

strength values. (ii) The selection of cell size V_0 does not play role in the determinating of the Weibull shape parameter m. (iii) Location parameter σ_u is a strong function of the cell size V_0 chosen. The drop of σ_u with increasing of V_0 is approximately the same for both types of microstructures. The value of V_0 must be arbitrary chosen to respect the real micromechanisms controlling the cleavage nucleation and propagation of microcrack within the elementary cell. (iiii) For both lower and higher values of cell size the failure features can be find out in fracture surfaces. The smaller value corresponds to to cleavage event within the one to two ferritic grains whereas the highest cell size corresponds to set of ferritic and austenitic grains ordered and acting similarly as in composite materials. According to experimental observation [14] the higher values of the cell size V_0 is recommended as the DSS behaviour in lower shelf corresponds more to composite materials than to standard steel.

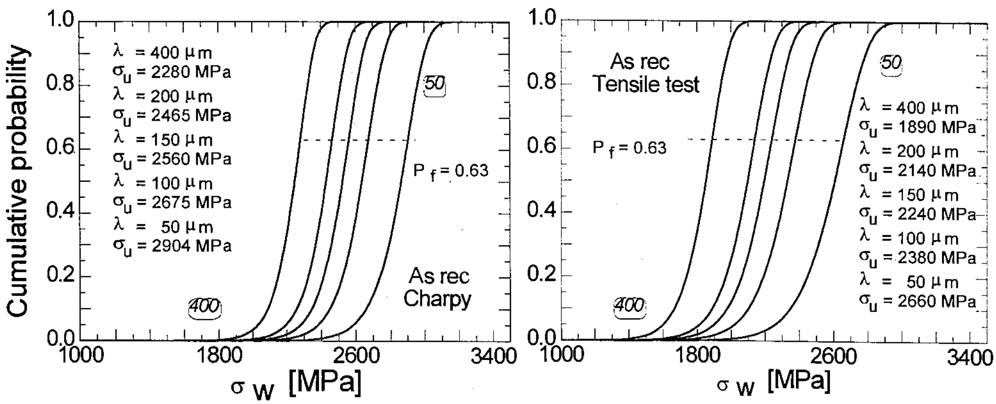

Figure 4: Curves of cumulative probability of (brittle) fracture for data obtained using a) Charpy type specimens and b) notched tensile specimens for as received material.

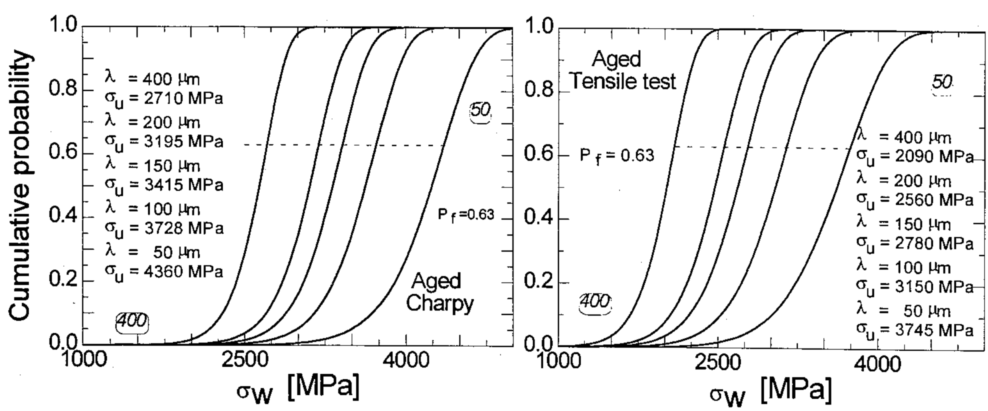

Figure 5: Curves of cumulative probability of (brittle) fracture for data obtained using a) Charpy type specimens and b) notched tensile specimens for aged material.

In order to test the reliability of determined local parameters the comparison of predicted fracture toughness - temperature diagrams (including scatter bands) with those obtained experimentally have been carried out. Procedure described in work [15] was applied for calculation. The final results are summarised in Fig. 6. The prediction calculated for cell size 50 and 400 μm yields to quite reasonable results. It is interesting that local parameters are not so dependent on cell size as in case of low alloy steel [16] and for both values of cell size nearly comparable prediction were received.

Brittle fracture behaviour

The forged thick wall steel is especially tough and exhibit notch impact toughness of nearly 200 J at room temperature. This tough behavior is retained even at low temperatures. The satisfactory level of fracture toughness values is retained to temperatures as low as -80 °C. The lowest values observed close to liquid nitrogen temperatures are higher than 80 MPam1/2. No dependence on specimen and crack plane orientation was found out (see data in Table 4, in which letter C represents tangential orientation, similarly L - longitudinal, R - radial).

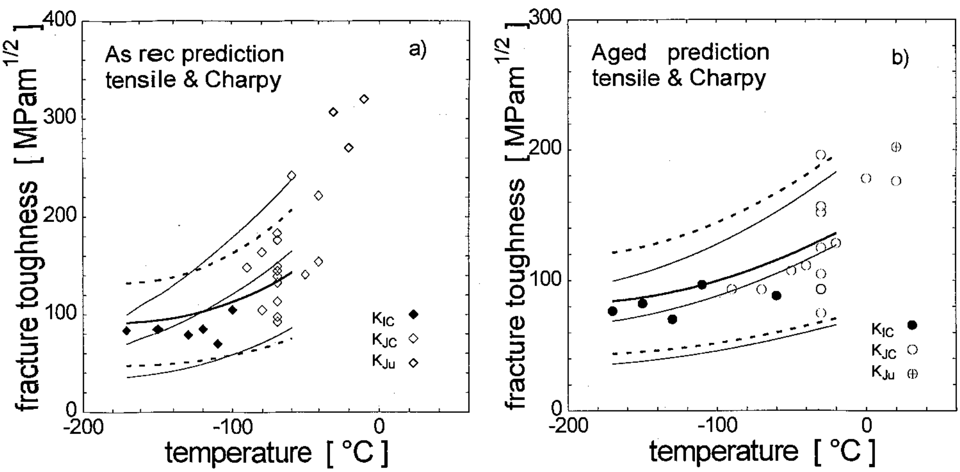

Figure 6: Prediction of fracture toughness - temperature dependencies from local parameters determined for a) as received steel and for b) aged steel and both notched specimen used

Fracture takes place in several steps. First, cleavage cracks are initiated in ferrite. These cleavage cracks cross ferrite and stop at the interface with austenite. Nevertheless, only the grains having a favorable orientation will lead to cleavage cracks in ferrite. After this stage, cracks subsequently grow by plastic deformation of austenite. It was shown that the cleavage nucleation is controlled by the plastic deformation in [10].

According to this observation, common for almost all investigated duplex steels [7], model and fracture criteria based on critical shear stress were developed. Principal stress distribution giving quite comparable values of σ_I^{max} independently of specimen geometry and comparable values of critical fracture stress as obtained experimentally [14] show that in lower shelf region the critical fracture stress criterion can be applied for fracture initiation condition although some amount of local deformation is necessary (Table 4). Nearly comparable values of critical fracture stress for both the as received and aged material mean that the resistance of microstructures against ferrite cleavage is comparable. This finding shows that equivalency of low temperature embrittlement and embrittlement due to age hardening [12] have its physical nature and differences between fracture behaviour are fully controlled by yield strength level.

Table. 4: Brittleness transition temperatures and critical fracture stress obtained using low blow impact tests and maximum tensile stress below notch root calculated for Charpy type and notched tensile specimen tested statically.

specimen axis	t_{GY} [°C]	t_{GY} [°C]	σ_F [MPa]	σ_F [MPa]	σ_F Charpy [MPa]	σ_F tensile [MPa]
longitudinal	- 90 (C)	-100 (R)	1820 (C)	1890 (R)		
tangential	-110 (R)	- 95 (L)	1900 (R)	1890 (L)		
radial	-105 (C)	- 95 (L)	1900 (C)	1880 (L)	2111	1867

4. CONCLUSION

Fracture behaviour was analyzed arising from temperature dependencies of static bend test of CVN specimen and static test of notched tensile specimen. Standard fracture toughness tests using CT specimen were carried out applied to test the validity of prediction calculated applying local approach concept. The following basic knowledge follow from investigation:

1. Although fracture behavior of duplex steel at lower shelf region and in embrittled condition suppose behavior of composite materials, local approach concept can successfully used for prediction of fracture behaviour

2. Slight dependence of prediction procedure on cell size was found, the higher values (close to 0.4 mm) of cell size fit to real fracture micromechanism in better way than lower values.

3. Prediction in lower shelf region have shown relatively poor correlation with measured data (in comparison to transition region). This is probably du to anomalous high fracture toughness in lower shelf region even at liquid nitrogen temperatures due to specific compensation of austenitici part of microstructure.

4. Comparable values of maximum tensile stress below notch for both notched specimen used and values obtained by experimental way from Charpy type specimen supposing validity of slip line field theory show that the critical fracture stress criterion can be used for assessment of brittlefracture behaviour of DSS (in lower shelf region and/or in embrittled condition)

ACKNOWLEDGMENTS

This research was financially supported by grant No. 101/97/1045 of the Grant Agency of the Czech Republic and grant No. A 2041701 of the Grant Agency of the Academy of Sciences.

REFERENCES

1. J. Charles, *Proc. of Duplex Stainless Steels*, Beaune, 1991, p. 3.

2. J. Charles, *Proc. of Duplex Stainless Steels*, Glasgow, TWI, 1994, p. KI.

3. J.O.Nilsson, *Materials Science and Technology*, 6, 1992, p. 685.

4. A. Pineau, P. Joly, In: *Defect Assessment in Components...*, ESIS/EGF 9, 1991, p. 381;

5. M. Lindnmo, *Proc. of Duplex Stainless Steels*, Beaune, 1991, p. 1289.

6. M. Liljas, *Proc. of Duplex Stainless Steels*, Glassgow, 1994, p. KV;

7. T. J. Marrow, A.O. Humpreys, M. Strangwood, *Fatig. and Fract. of Engng. Mat...*, in print.

8. P. Joly, A. Pineau, *Scand. Journ. Of Metallurgy*, 1995, 24, 226-236.

9. F. M. Beremin, *Metall. Transaction Vol. 14A* (1983), 2277-2287.

10. C. Sainte-Catherine, *Meeeting of ESIS TC1, Elastic Plastic Fract. Mech., Appen.1,* (1995).

11. C.S. Wiesner C. S., *Meeting of ESIS TC1*, Elastic Plastic Fracture Mechanics, P2, (1995).

12. I. Dlouhý, V. Kozák, M. Holzmann, *Steel Research* (1997), to be published

13. V. Kozák J. Malý, *J. Engineering Mechanics 3,* (1993), 46-52.

14. I. Dlouhý, V. Kozák, M. Holzmann, *Proc. of ECF 11,* Futuroscope, (1996) 651-656.

15. D.P.G. Lidbury , et al.: *TAGSI Symp. Advanced in Fracture Mechanics*, (1996).

16. I. Dlouhý, V. Kozák et al.: *Journal de Physique IV*, Colloque C6, Vol. 6, (1996), 205-214.